Asia-Pacific Magnetic Recording Conference 2016
13 July – 15 July 2016, Yonsei University, Korea

Acoustic Noise of Spindle Motor Induced By Electromagnetic Torque Ripple

Kun Xia, Jing Lu *, Bin Dong, Chao Bi

Department of Electrical Engineering, University of Shanghai for Science and Technology, Shanghai, China

Abstract—**The torque ripple of is one of the major sources inducing vibration and noise in brushless DC motor, and this is special concerned in many applications like the spindle motor used in hard disk drive. However, the relationship between the torque ripple and acoustic noise/vibration is quite complicated. This paper presents the way to investigate such a relationship. The sound pressure spectrum of the acoustic noise is used to analyze the effects of torque ripple of different drive modes. The testing results show that, this spectrum is very helpful in designing the high performance spindle motor drive mode.**

Index Terms – BLDC motor, spindle motor, acoustic noise, torque ripple, drive mode

I. INTRODUCTION

Brushless DC (BLDC) motors make themselves attractive in industrial applications for its many advantages. However, torque ripple is the worst drawback which results in mechanical vibration and acoustic noise [1].

Acoustic noise sources may be categorized into mechanical and electromagnetic ones for the BLDC motor. The mechanical noises include the ones caused by the windage friction of the rotor surface and the rolling of bearing balls rotating at high speeds; the electromagnetic (EM) noises are considered to be formed by unbalanced magnetic pull (UMP) [2] and torque ripples [3, 4]. Acoustic noise resulting from the motor deformation induced by the radial magnetic field, may also be considered as the EM noise [5].

UMP is determined by EM structure of the motor, the quality of the component, and the quality of motor assemblage. The noise from UMP may be reduced to a minimal value with fine motor design and precise production technology [6]. Moreover, for BLDC motors with no less than 5 magnetic pole-pairs, the deformations of tested motors caused by the drive current could be neglected [7].

Torque ripples in the BLDC motor consist of cogging torque and operation torque ripples. Cogging torque is a common defect in permanent magnet motors, and can be minimized via better motor design [8]. Operation torque ripple can be classified into commutation torque ripple and inherent torque ripple; the inherent torque ripple present at steady conduction state. Methods of commutation torque-ripple reduction have been developed in references [9]. The effects of non-ideal back-EMF waveform and the reduction method of inherent torque ripple have been discussed in reference [10].

However, the exact observation of the torque ripple is more difficult when the sampling frequency is much lower than the switching frequency. The torque estimation method which primarily used in direct toque control (DTC), is difficult to use when the parameters of the motor keep changing in rotation. In practice, torque sensor is also unfit to be used in torque ripple measurement for the less of frequency response in high speed regions. In recent years, researchers have proposed new methods to measure torque, for example fiber grating, differential magnetic and surface acoustic wave [11], but these methods are too complicated for practical use.

The EM acoustic noise formed by EM torque force takes the information of torque ripples, and is suitable for torque ripple detection when the BLDC motors operate at high speed or without load.

This paper studies the causes of EM torque ripple and introduces the production process of EM acoustic noise. Different torque ripples and acoustic noise in BLDC motor are analyzed. Three driving methods are employed in this research to illustrate the relationship between torque ripples and acoustic noise. One anechoic chamber is employed to acquire the quiet experiment environment. The results of acoustic experiments reveal the relationship between EM torque ripple and acoustic noise.

II. TORQUE RIPPLE IN BLDC MOTOR

There are many control strategy in BLDC driving system for three-phase star-connected windings motor, and the most popular one is six-step square-wave driving method. The dc-link voltage is constant, thus named as constant voltage driving mode (CV-mode) in this paper.

A. Commutation Torque Ripple

The ideal back-EMF waveforms shapes of BLDC motor e_a , e_b , and e_c are trapezoidal. When the stator windings of phase A, B, and C are fed with square wave currents, the EM torque force T_{em} on the motor shaft is constant and could be expressed as

$$T_{em} = \left(e_a i_a + e_b i_b + e_c i_c\right) \frac{1}{\omega_r} \tag{1}$$

where ω_r is the mechanical angular speed of the rotor.

The ideal back-EMF BLDC motor operating under CV-mode do not have inherent torque ripple. However, the expected square waveform current is hard to achieve for the current is impeded by motor stator inductance. The difference between rising and falling rates of the phase currents directly contributes to commutation torque ripple. The commutation torque ripple could reach 50% of average output torque. [8]

The conventional driving system for BLDC motor is presented in Fig. 1. The switching states of CV-mode are generated by the controller according to rotor position signals of hall position sensors. The PWM_ON scheme which has least commutation ripple compared with other PWM strategy is applied in this paper. Fig. 2a shows the phase current

waveforms and the gate signals on inverter switches in CV-mode at commutation interval when the phase current is changing from phase-AB to phase-AC. The current ripple appearing at commutation period contributes to the commutation torque ripple.

Considering the commutation is very quick, back-EMF is supposed to be constant during commutation. In the following, the commutation process of the phase current from phase-AB to phase-AC is analyzed. The current of phase B cannot immediately drop to zero at the beginning of the commutation, and flows through the freewheeling diode of T_3. The stator terminal voltage during the commutation interval can be illustrated as

$$\begin{cases} \dfrac{U_{dc}}{2} = Ri_a + L\dfrac{di_a}{dt} + e_a + U_{No} \\ \dfrac{U_{dc}}{2} = Ri_b + L\dfrac{di_b}{dt} + e_b + U_{No} \\ -\dfrac{U_{dc}}{2}(2D-1) = Ri_c + L\dfrac{di_c}{dt} + e_b + U_{No} \end{cases} \tag{2}$$

where U_{dc} is the dc-link voltage, D is the duty ratio of PWM on inverter switches, L is the phase equivalent inductance of the stator windings and can be calculated from the self-inductance L_s and the mutual inductance M for individual coils as $L = L_s - M$, and R is the stator winding resistance.

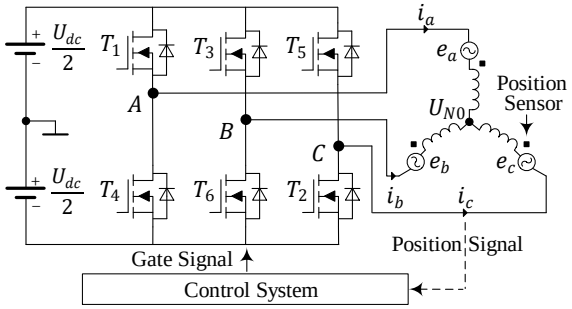

Fig. 1 Conventional driving system of BLDC motor.

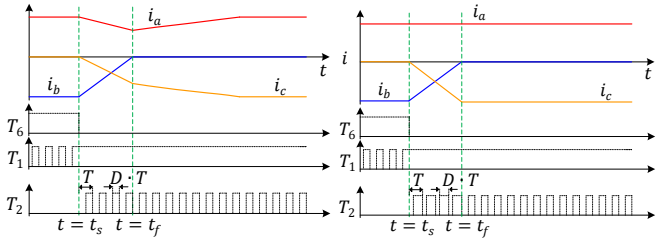

a. CV-mode *b*. VV-mode

Fig. 2 switching pattern and current waveforms of BLDC motor.

According to instantaneous power theory, the voltage of the motor neutrals point can be described as

$$U_{N0} = \left(\frac{3U_{dc}}{2} - DU_{dc} - e_a - e_b - e_c\right)/3 \tag{3}$$

It is assumed that the phase resistance is relatively small. Thus neglecting the influence of resistance then the current derivative of phase-A can be given by

$$\left\langle \frac{di_a}{dt} \right\rangle_{ts} = \frac{DU_{dc} - 2e_a + e_b + e_c}{3L} \tag{4}$$

At the beginning of commutation, the back-EMF of each phase can be expressed as $e_a = E_m$, $e_b = E_m$, and $e_c = -E_m$, where E_m is the amplitude of the back-EMF. From the torque equation, the rising and falling speed of the current should be equal to produce constant output torque during commutation period, and it always exists

$$DU_{dc} = 4E_m \tag{5}$$

that means the commutation torque ripple can be suppressed when the duty ratio of PWM maintains $4E_m / U_{dc}$.

Normally, D in the commutation interval should be larger than the duty ratio in the steady conduction state. When the needed D during commutation is greater than 1, the voltage boost converter should be applied in front of the inverter [12]. Utilizing this variable voltage driving mode (VV-mode), current ripple during the commutation can be minimized. Fig. 2b presents the phase current waveform and switching pattern of BLDC motor in VV-mode.

B. Inherent Torque Ripple

As shown in Fig. 2b, there is no torque ripple under the ideal trapezoid back-EMF. However, confined by the motor manufacture technology, the waveform of back-EMF is actually more quasi-sine-wave rather than trapezoidal-wave shapes, particularly when the BLDC motors run at high speeds. Affected by the non-ideal back-EMF, the current is no longer square-wave during conduction state which leads to the inherent torque ripple. Fig. 3 illustrates the phase current waveform under non-ideal back EMF in CV-mode. Where e_{ab} and i_a is the back-EMF of phase A to B and phase A current, respectively.

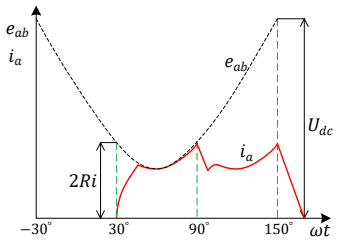

Fig. 3 Phase current under non-ideal back-EMF.

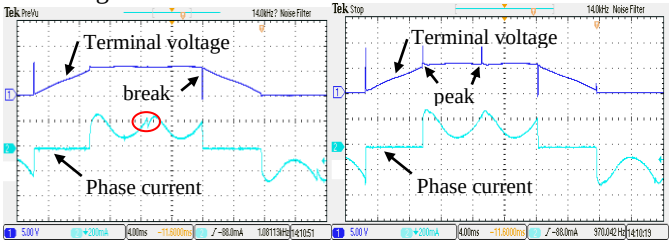

a. CV-mode *b*. VV-mode

Fig. 4 Measured waveforms when operating without load.

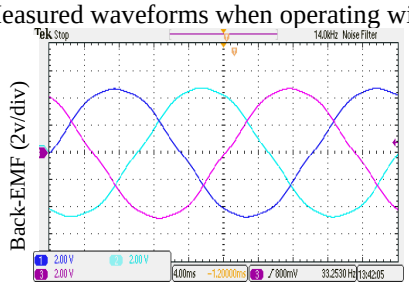

Fig. 5 Measured back-EMF waveform of BLDC motor.

The current ripple during conduction state would be high when the motor runs without load or with light load, because the ratio of the back-EMF voltage versus constant driving voltage would be high at high speeds. Although the commutation torque ripple suppression method is applied in driving system, the current ripple still exists at steady conduction state as shown in Fig. 4b, which contributes to high output torque ripple.

The break on the terminal voltage at the commutation interval is caused by the free-wheeling diode on the out-going phase. And the peak on the terminal voltage is generated by the boost converter in VV-mode. The current ripple marked with an ellipse in Fig. 4a resulting from BLDC motor commutation can be reduced in VV-mode as shown in Fig. 4b. The back-EMF waveforms of the prototype motor running without currents in stator windings is presented in Fig. 5. It resembles a poorly-shaped sinusoidal. However, the space vector driving mode (SV-mode) may eliminate both inherent and commutation torque ripple of permanent magnet motors which have the sinusoidal back-EMF waveform. [4]

III. Acoustic Noise Source of BLDC Motor

Neglecting airflow noise, the acoustic noise in BLDC motor mainly includes electromagnetic ones and mechanical ones. EM noise in BLDC motor is primarily caused by the EM force which exists in air gap and provides the circle power. The vibration of the stator under the EM force pressure transmits to the air and generates acoustic noise.

The BLDC motor commutates every 60 degrees in one electrical cycle in CV-mode and VV-mode. The commutation and inherent torque ripple will appear in each commutation process when the motor runs without load on shaft. These torque ripples give rise to the EM acoustic noise, thus the fundamental frequency of acoustic noise from torque ripple could be calculated using the commutation frequency of BLDC motor as

$$f_{i^{th}} = i \times k \times p \times \frac{n}{60} \quad i=1,2,3... \tag{6}$$

where $f_{i^{th}}$ is the i^{th} order harmonics of motor commutation frequency, i is the number of harmonics order, k is the steps of commutation in one electrical cycle, p is the stator pair of poles, and n is the rotational speed(r/min). In CV-mode and VV-mode, $k=6$, thus the fundamental commutation frequency is $0.1pn$.

Mechanical noise of BLDC motor mainly comes from the rolling of bearing balls. Then the fundamental frequency of mechanical noise is

$$f_s = \frac{n}{60} \tag{7}$$

The BLDC motor system resonates as a frequency of excitation force components moving close to any of its axial resonant frequency. The resonant frequency is inherent in the motor and determined by motor structure. If considering the motor as an elastic system, the resonant frequency can be expressed as

$$f_c = \frac{1}{2\pi}\sqrt{k_s / m} \tag{8}$$

where k_s is the stiffness and m is the mass of the elastic system.

The vibration of motor system principally originates from the stator, and the EM force directly functions on the cogging and magnet, the fundamental resonant frequency of stator may be calculated as

$$f_{c0} = \frac{1}{2\pi}\sqrt{\frac{Eh_j}{m' R_j^2}} \tag{9}$$

where h_j and R_j is the radial height and average radius of the stator yoke, respectively. m' is the surface mass on the average radius of the stator yoke, and E is the elastic modulus.

The acoustic noise is obtained through the sound level meter and recorded by the test software on PC. The spectrum of the sound pressure level (SPL) can be obtained via Matlab math calculation. In order to accurately measure the acoustic noise, the sound pressure at several points are measured in an anechoic chamber. The eight points surrounding the tested motor are shown in Fig. 6. The distances of each test points from the motor as the center are 20 cm. From the SPL of eight selected test points, the average SPL of the tested motor at the distance of 20 cm could be calculated as

$$\overline{L_p} = 10\log\left\{\frac{1}{N}\left(\sum_{i=1}^{N} 10^{\frac{L_{p,i}}{10}}\right)\right\} \tag{10}$$

where $\overline{L_p}$ is the average SPL of tested BLDC motor, and $L_{p,i}$ and N is the SPL at each point and the number of measurement points.

The acoustic noise testing system is given in Fig. 7. The tested motor and microphone are placed in the anechoic chamber. One recording interface is applied to acquire sound signals from the microphone to be stored in the PC. The experimental system also includes DC voltage power, driving circuit, and oscilloscope. The SPL spectrum of the background noise in the anechoic chamber is shown in Fig. 8a.

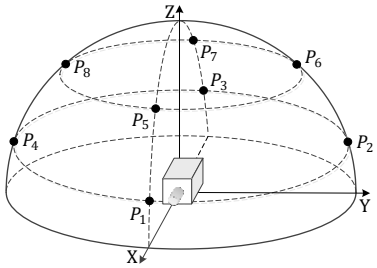

Fig. 6 Selected points for measuring SPL of BLDC motor.

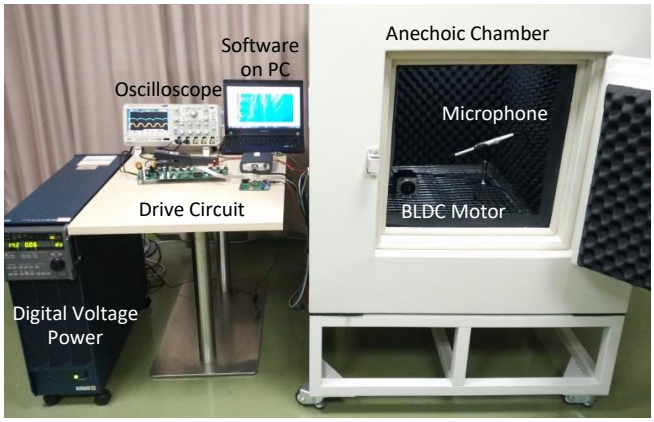

Fig. 7 Experimental system of acoustic noise measurement

IV. Experiments of BLDC Motor Acoustic Noise

The important parameters of the prototype motor are shown in table 1. The frequency of PWM is 30 kHz, which is much higher than 20 kHz to avoid the introduction of external interference.

The acoustic noise of BLDC motor is affected by both commutation and inherent torque ripple in CV-mode. SPL spectrum of test point P_2 for tested motor is shown in Fig. 8b. The range of the SPL spectra is from 0 to 20 kHz. Meaningful testing data is marked with two ellipses in Fig. 8b compared with background noise SPL spectrum.

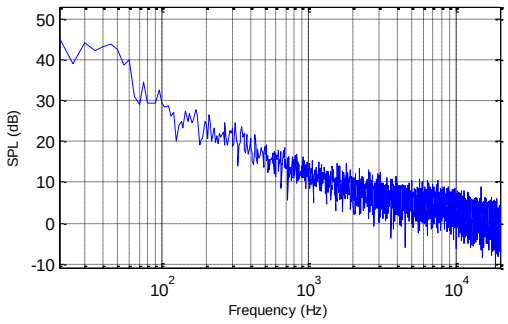

a. Anechoic chamber background noise

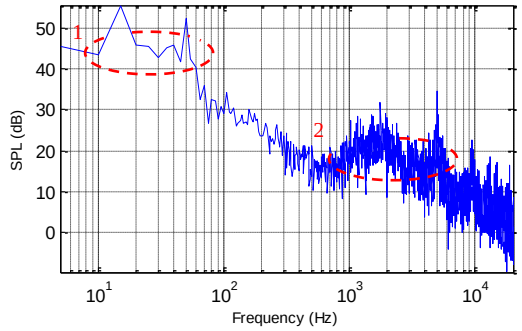

b. Driving with CV-mode

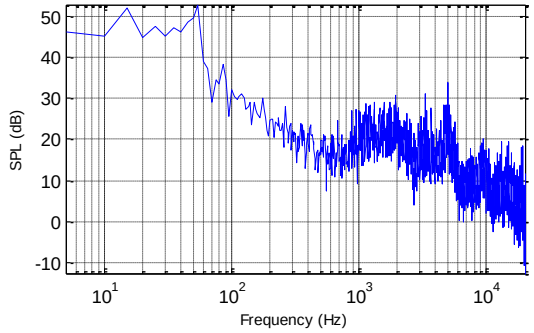

c. Driving with VV-mode

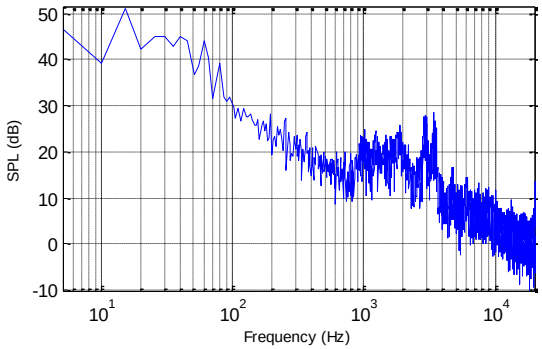

d. Driving with SV-mode

Fig. 8 SPL spectrum for BLDC motor

When the rotating speed is 1000 r/min and the fundamental frequency of commutation f_1^{th} is 500 Hz in CV-mode and VV-mode. Mechanical noise in the low frequency level of the motor sound amplitude spectrum varies from fundamental frequency 18 Hz to 5 order harmonic frequency 90 Hz as marked with the first ellipse in Fig. 8b. The second ellipse shows the EM noise of the BLDC motor from f_1^{th} to f_{11}^{th} which is in the high frequency level from 500 to 6000 Hz. The corresponding sound amplitudes of two ellipses are shown in Fig. 9.

TABLE I
PARAMETERS OF THE BLDC MOTOR

Parameters	Value
Rated Voltage (V)	36
Rated Power (W)	200
Rated Speed (r/min)	2000
Rated Torque (N.m)	0.8

Pole Pairs	5
Phase Resistance (Ω)	0.2
Phase Inductance(μH)	395.3

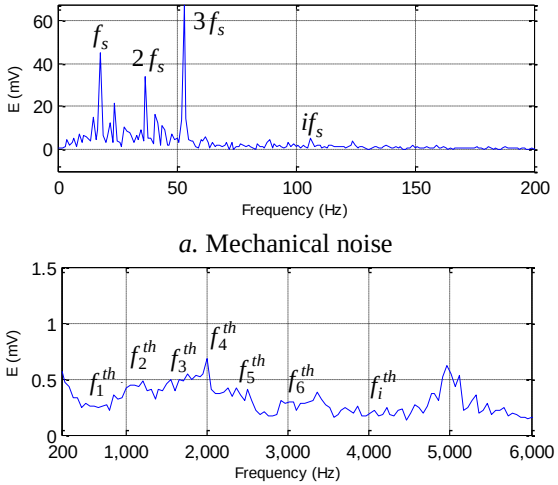

a. Mechanical noise

b. EM noise

Fig. 9 Sound amplitude spectra

The commutation torque ripple can be suppressed significantly when the motor driving with VV-mode, and the inherent torque ripple is reduced a little. SPL spectrum of the measuring point P_2 in VV-mode is shown in Fig. 8c.

Frequency of mechanical and EM noise in VV-mode share the same range on SPL spectrum as in CV-mode. Comparing Fig. 8b and 8c, the EM noise does not show a significant reduction when the motor driving with VV-mode, while mechanical noise reduces slightly. Further, concluding the commutation torque ripple is not the only source which contributing to EM acoustic noise when the BLDC motor at no-load condition.

In practical, the back-EMF waveforms are always non-ideal shapes, hence SV-mode which is usually used in PM motor driving, does not have commutation ripple and can significantly reduce the inherent torque ripple. SPL spectrum in SV-mode of the P_2 measuring point is shown in Fig. 8d. The SPL value of each point is shown in Table 2. The average SPL of the tested motor in SV-mode is 45.57 dB, which is much lower compared with the noise in CV-mode and VV-mode. It indicates that torque ripple directly contribute to EM noise and give rise to mechanical noise ultimately.

TABLE II

MEASURE SPL OF EACH POINT-Noise (dB)

Point	CV-mode	VV-mode	SV-mode
P_1	52.4	51.6	45.2
P_2	53.8	53.4	47.9
P_3	53.4	53.7	46.0
P_4	54.7	53.8	46.2
P_5	46.8	46.6	45.2
P_6	47.4	46.7	42.0
P_7	48.7	47.3	47.0
P_8	45.5	44.9	41.2

$\overline{L_p}$	51.54	51.03	45.57

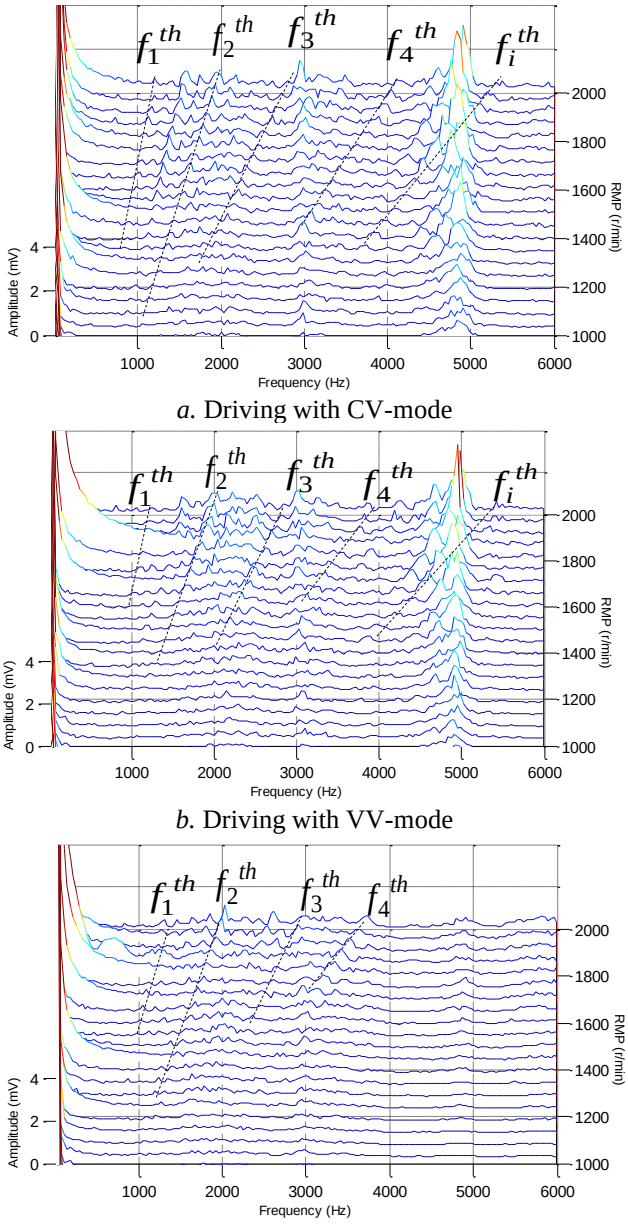

a. Driving with CV-mode

b. Driving with VV-mode

c. Driving with SV-mode

Fig. 10 Acoustic noise spectra waterfalls

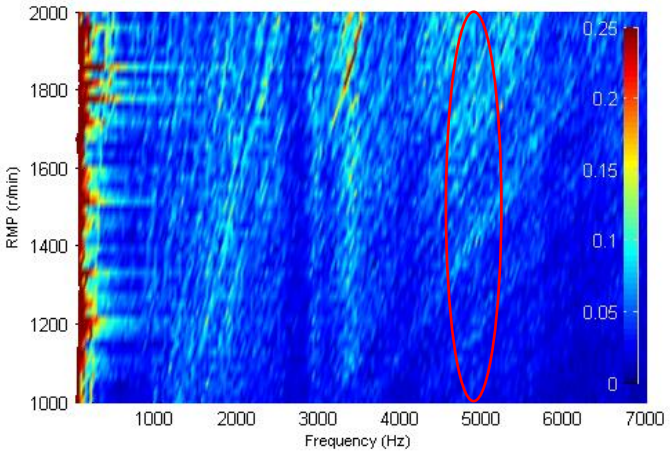

Fig. 11 Waterfall of EM acoustic noise amplitudes

Considering the influence of the motor speed, the measured acoustic noise vs motor speed driven in the CV-mode, VV-mode, and SV-mode are shown respectively in Fig. 10 with waterfall format. The smooth section from 6 kHz to 20 kHz is ignored and not given in Fig. 10 to focus on meaningful details. It is known that the torque ripple in SV-mode is the minimum and that in CV-mode is the maximum among these three driving methods. The amplitude of commutation frequency points marked with dotted line in each subfigure of Fig. 10 is proportional to the torque ripple in different driving modes. It is proved that the torque ripple in BLDC motor is related to the amplitudes of specific frequency points in acoustic noise spectra, and these frequency points can be calculated from (6).

Amplitudes of acoustic noise are much higher at approximately 5000 Hz for all rotating speeds as highlighted with an ellipse in Fig. 11. It is the resonant frequency as illustrated in (9). While enough experiments data are collected, the relationship between the variation of the acoustic noise and the torque ripple could be set up according to a scientifically defensible mathematical model or an approximate estimation.

V. CONCLUSION

From the experiment results of this paper, the EM acoustic noise in the tested BLDC motor is mainly caused by the EM torque ripple. And the related frequency points to the torque ripple are shown in the waterfalls of acoustic noise spectra. Due to the non-ideal back EMF, the inherent torque ripple has much more effects on the EM torque ripple than the commutation torque ripple when the motor at no-load condition. However, the space vector driving strategy, which can eliminate most torque ripple in BLDC motor, has the lower acoustic noise than the other two driving methods. Using these relative frequency points, the torque ripple can be estimated from motor acoustic noise in further researches.

ACKNOWLEDGMENT

This work was supported in part by the National Natural Science Foundation of CHINA under Grant 51207091.

REFERENCES

[1] S.A. Saied et al, “Cogging torque reduction in brushless DC motors using slot-opening shift”, *Advances in Electrical & Computer Engineering*, vol. 9, no. 1, 2009

[2] D.M. Ionel et al, “Assessment of torque components in brushless permanent-magnet machines through numerical analysis of the electromagnetic field”, *IEEE Transactions on Industry Applications*, vol. 41, no. 5, 2005

[3] D. Torregrossa et al, “Prediction of acoustic noise and torque pulsation in PM synchronous machines with static eccentricity and partial demagnetization using field reconstruction method”, *IEEE Transactions on Industry Electronics*, vol. 59, no. 2, 2011

[4] P.G Scholar, “Analysis and experimental investigation to mitigate mechanical vibration and acoustic noise in direct torque controller fed PMSM”, *International Journal of Research in Engineering and Technology*,vol.3, no.7, 2014

[5] J.H. Leong et al, “Acoustic noise and vibration of direct-torque-controlled permanent magnet brushless DC drives”, *Power Electronics, Machines and Drives conf.*, Bristol, England, March 2012

[6] S. Sung et al, “Effect of additional harmonics of driving current on torque ripple and unbalanced magnetic force in HDD spindle motors with stator and rotor eccentricity”, *Microsystem Technologies*, vol. 21, no. 12, 2015

[7] S. Lin et al, “Analysis of acoustic noise sources of FDB and ADB spindle motors operating at BLDC mode”, *IET conference on Power Electronics. Machines and Drives*, York, England, April 2008

[8] S.K. Chang et al, “New cogging-torque reduction method for brushless permanent-magnet motors”, *IEEE Transactions on Magnetics*, vol. 39, no. 6, 2003

[9] Y.K. Lin et al, “Pulsewidth modulation technique for BLDCM drives to reduce commutation torque ripple without calculation of commutation time”, *IEEE Transactions on Industry Applications*, vol. 47, no. 4, 2011

[10] J.C. Fang et al, “Torque ripple reduction in BLDC torque motor with nonideal Back EMF”, *IEEE Transactions on Power Electronics*, vol. 27, no. 11, 2011

[11] P. Kampmann et al, “Integration of Fiber-Optic sensor arrays into a Multi-Modal tactile sensor processing system for robotic End-Effectors”, Sensors, vol. 14, no. 4, 2014

[12] V. Viswanathan et al, “Approach for torque ripple reduction for brushless DC motor based on three-level neutral-point-clamped inverter with DC–DC converter”, IET Power Electronics, vol. 8, no. 1, 2015

[13] K.S. Ha et al, “Design and development of brushless variable speed motor drive for low cost and high efficiency”, *IAS Annual Meeting Conf*, 2006